Experiments on superfluid ^{4}He evaporation

S. Balibar, J. Buechner, B. Castaing, C. Laroche, and A. Libchaber
Groupe de Physique des Solides de l'Ecole Normale Supérieure, 24 rue Lhomond, 75231 Paris 05, France
(Received 10 March 1977)

A study of the evaporation of superfluid ^{4}He, using the heat-pulse technique, is presented; working at low temperature, $0.1 < T < 0.6$ °K, the phonon and the roton fluids are decoupled. We observe atoms evaporated by a phonon second-sound pulse between 0.4 and 0.6 °K. The temperature dependence of the signal is interpreted by a simple model where one phonon of energy E emits one atom of energy $E - E_0$ ($E_0 = 7.15$ °K is the atomic binding energy in the liquid). At lower temperature, down to 0.1 °K, a ballistic-phonon regime is observed, associated with no detected evaporation. Concerning rotons, we observe well-defined signals due to atoms evaporated by them. Analyzing the arrival time as a function of the liquid path, we propose an evaporation process such as one roton of energy E emits one atom of energy $E - E_0$. This leads to a minimum kinetic energy of 1.5 °K for the evaporated atoms, effectively observed. An estimation of the roton mean free path is deduced and a maximum roton velocity of 160 ± 10 m sec^{-1} is observed.

I. INTRODUCTION

After the experiment by Johnston and King,[1] the theoretical predictions by Anderson,[2] and various other theoretical and experimental contributions,[3–5] an important question still remains open: Do single elastic emission processes such as those suggested by Anderson contribute to the evaporation, i.e., 1 phonon (energy E) $\rightarrow$ 1 atom ($E - E_0$) and 1 roton (E) $\rightarrow$ 1 atom ($E - E_0$), where $E_0 = 7.15$ °K is the atomic binding energy?

We present here new experimental results on the evaporation from superfluid ^{4}He at low temperature ($0.1 < T < 0.6$ °K). In this experiment, where we propagate a heat pulse through a liquid-gas interface at low temperature, phonons and rotons are decoupled in the liquid and the atoms move ballistically in the gas.[6] The phonons created by the heater propagate through a few millimeters of liquid and arrive first on the free surface, where they evaporate atoms which are detected by a bolometer in the gas. The rotons of lower velocity evaporate atoms later and we thus separate the two contributions to the evaporation.[3] We interpret the two signals due to atoms evaporated respectively by phonons and rotons in terms of Anderson's processes.

The paper is organized as follows: In Sec. II, we describe the experimental arrangement. In Sec. III we present the experimental results concerning the evaporation by phonons in the second-sound-like regime. The results can be analyzed by a simple model involving the process: 1 atom (E) evaporates 1 atom ($E - E_0$). We also present some data on the phonon propagation itself, which seem to be more and more ballistic as the temperature goes down to 0.1 °K. In the low-temperature regime ($T < 0.3$ °K), we have not been able to detect atoms evaporated by phonons.

In Sec. IV, we study the evaporation by rotons coming up to the free surface. Performing a time-of-flight experiment, we analyze the arrival time of the signal as a function of the level of the liquid, which can be displaced from the heater up to the detector. This confirms first the ballistic character of the propagation of rotons. Moreover, this gives evidence for an evaporation process [1 roton (E) evaporates 1 atom ($E - E_0$)], which involves a minimum kinetic energy of 1.5 °K for the evaporated atoms, the minimum roton energy being 8.65 °K. The analysis of the signal amplitude gives an estimate of the roton mean free path, about 3 mm for rotons of velocity 70 m sec^{-1}. Finally, in Sec. V, we present a surprising result concerning the rotons: the evaporation data lead to a maximum velocity of the rotons in the liquid of 160 ± 10 m sec^{-1}.

II. EXPERIMENTAL TECHNIQUES

In a heat-pulse experiment, a heater and a heat detector are placed at the boundaries of the medium where the experiment is taking place. In our experiment, the heater is a thin metallic film. A voltage pulse is applied to it at time zero. The detector is a temperature-dependent resistant film, whose resistance is measured as a function of time after time zero, when the heater signal is applied. The experimental arrangement is schematized in Fig. 1. The heat pulse propagates vertically over a fixed distance of 8 mm for some experiments and 6.85 mm for the others. The level of the free liquid surface can be displaced from below the heater to above the detector,

using a moving plunger. The height of this level is measured using a cylindrical capacitor, with an absolute precision of 50 μm. The experiment is performed in a ^{3}He refrigerator down to 0.4 °K, and a ^{3}He-^{4}He dilution refrigerator down to 0.1 °K. The temperature of the helium experimental chamber is regulated with a precision of 10^{-5} °K. In the ^{3}He apparatus, the moving plunger is suspended by a small wire which goes up to the ambient temperature; in the dilution apparatus, it is attached to a soft iron cylinder moving in the field of a small superconducting coil. A 3-mm-thick superconducting lead slab magnetically shields the heater-detector system from all stray fields. The heater is a Cu or Au film evaporated on a glass substrate of typical resistance 25–50 Ω. Its thickness is 300–500 Å; its shape is that of a serpentine with a 0.1 mm width and 1 cm length. The detectors are superconducting films polarized in the middle of their superconducting transition by a vertical magnetic field. This field is produced by a solenoid immersed in the outer ^{4}He Dewar. Various types of detectors have been used; we started first with Al detectors, evaporated on a glass substrate, a shape similar to the heater, with a typical normal resistance of 60 Ω and a sensitivity of about $(1/R)(dR/dT) \simeq 5$ °K^{-1} at $T = 0.6$ °K, where R is the detector resistance.

We then used Zn films, 1000 Å thick, evaporated on glass with a 100-Å Au underlayer and a normal resistance of 18 Ω, sensitivity $(1/R)(dR/dT) = 60$ °K^{-1} at 0.5 °K. At low temperature, below 0.2 °K, the detector response time was too long, typically 40 μsec at 0.1 °K. Finally, in order to have a sensitive detector at low temperature, we used a 2000-Å Zn film evaporated on a Si single crystal with a 1000-Å SiO underlayer. Such a structure had a response time faster than 1 μsec at 0.1 °K, and a sensitivity of about 60 °K^{-1}, a normal resistance of 4 Ω.

The resistance of the detector is measured as a function of time using a small polarization constant current ($I < 0.2$ mA to avoid superfluid film flashing) and a boxcar integrator. We used pulses of 1 μsec duration, 0.1–3-V amplitude, and a 200-Hz repetition rate.

The experimental chamber is filled with ^{4}He of normal isotopic purity 10^{-7}. We start from gaseous helium and condense it slowly through a superleak filter of 0.1 μm size.

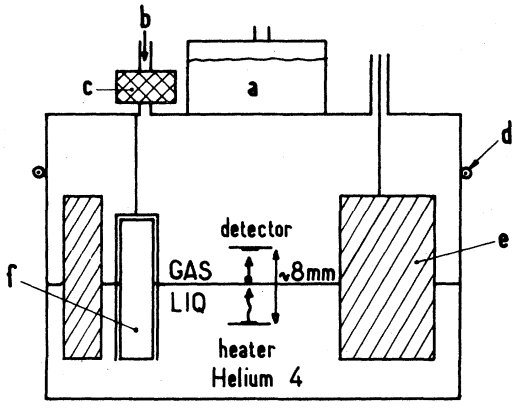

FIG. 1. Experimental arrangement: (a) ^{3}He Dewar; (b) ^{4}He capillary; (c) superleak; (d) thermal regulation; (e) moving plunger; (f) cylindrical capacitor.

III. EVAPORATION BY PHONONS

As shown in a preceding publication,[3] we can separate the contribution of phonons and rotons to the evaporation of He atoms. At low temperature, $T < 0.6$ °K, the phonons and rotons generated by the heater are decoupled,[7] as the phonon-roton collision time τ_{pr} becomes greater than a flight time from heater to detector. The phonons are faster and arrive first at the detector.[8] In this section, we will concentrate on a phonon signal ($t < 100$ μsec). In Fig. 2 one can see four different signals recorded at four different temperatures. We define the two situations A and B as follows:

A: the liquid level is above the detector; the signal

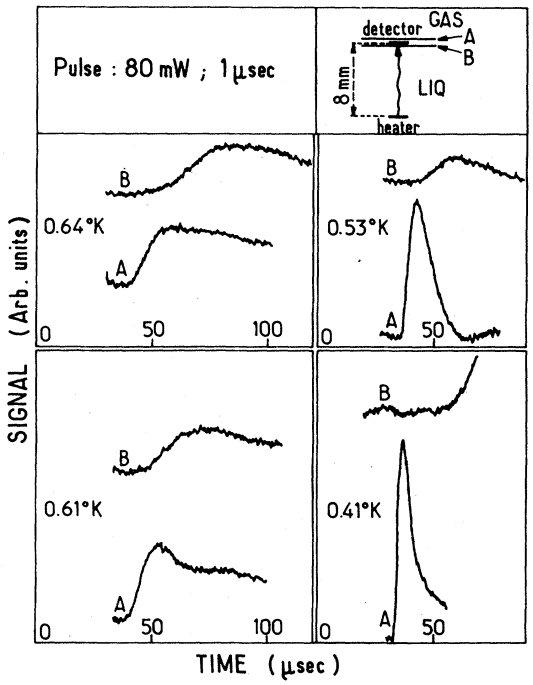

FIG. 2. Various phonon signals vs time recorded at four different ambient temperatures T (0.64 to 0.41 °K) in two different experimental situations A and B. As schematized in the upper-right corner, A corresponds to a liquid-gas interface above the detector, B to an interface just below (less than 50 μm). B signals arrive a little later than A signals. The amplitude ratio $R = B/A$ decreases as T decreases.

is due to direct arrival of phonons following a complete liquid path.

B: the liquid level is just below the detector and the signal is due to atoms evaporated by the phonon pulse. The gas thickness, less that 50 μm, is negligible compared to the liquid one, 8 mm, so that the arrival time is only related to the liquid path. The detector sensitivity is the same in situation *A* and *B*; three main observations can be inferred from Fig. 2.

(i) The *A* signals have a changing line shape and a faster velocity as the temperature varies from 0.64 to 0.41 °K. This behavior is associated with a transition in the mode of propagation from a phonon second sound to ballistic phonons. This transition is well known,[9] and occurs when the mean phonon-phonon collision time τ_{pp} becomes of the order of the flight time from heater to detector. The velocity of a pure phonon second sound is $V_1 = c/\sqrt{3} = 137$ m sec^{-1}. For a point source and a point detector, the amplitude of the received signal is proportional to the derivative of the excitation,[10] i.e., an *s*-like shape with a negative (cold part) behind a positive (hot) part. (This *s*-like shape is not obvious on the early recordings of Fig. 2, where the base line was not horizontal but can be seen unambiguously on the bottom curve of Fig. 4.)

At lower temperature, we observe a quasiballistic-phonon pulse, with a positive amplitude and propagating at a velocity close to the sound velocity ($c = 238$ m sec^{-1}).

(ii) The amplitude ratio $R = B/A$ of the *B* to the *A* signals decreases as the temperature decreases.

(iii) The *B* signals arrive slightly later than the *A* signals.

All this behavior can be explained by the following simple model: The *B* signals are due to the evaporation of atoms by the high-energy phonons lying in the second-sound-like part of the pulse, i.e., phonons with energy *E* larger than $E_0 = 7.15$ °K. In the phonon pulse, the starting edge is related to low-energy phonons, phonons of longer mean free path, escaping from the pulse in the forward direction. The longer time part of the pulse is mainly related to interacting phonons creating a second sound; the phonons are there in thermal equilibrium and a high-energy exponential tail in the phonon distribution is always present.

The high-energy phonons are able to evaporate atoms, but arrive later at the free surface: this is the qualitative reason for observation (iii).

Concerning observation (ii), Fig. 3 shows that the ratio $R = B/A$ of the peak heights of signals *B* and *A* (×, +, and ○ correspond to various experiments) decreases as a function of $1/T$ roughly according to $e^{-7.15/T}$ (dashed line). The full line corresponds to the equation

$$R = R_0(\epsilon_0^4 + 4\epsilon_0^3 + 12\epsilon_0^2 + 24\epsilon_0 + 24)\exp(-\epsilon_0) \quad , \qquad (1)$$

where R_0 is an adjustable parameter and $\epsilon_0 = E_0/T = 7.15/T$. Equation (1) fits very well with the experimental points and is obtained after a simple calculation assuming four strong hypothesis: (a) evaporation processes like one phonon $(E) \rightarrow$ one atom $(E - E_0)$, (b) a transmission factor α at the liquid-gas interface like

$$\alpha = 0 \quad \text{for } E < E_0 \ ,$$

$$\alpha = \alpha_0 \quad \text{for } E > E_0 \ ,$$

(c) a thermal equilibrium of phonons in the pulse at a temperature $T + \Delta T$, where $\Delta T \ll T$ and T is the ambient temperature, and (d) an energy-independent transmission factor for phonons at the helium-aluminum detector interface.

R is then easy to estimate: it represents the ratio of the energy of high-energy phonons divided by the total energy of the pulse

$$R = \int_{E_0}^{+\infty} E^4 T^{-2} e^{-E/T} dE \Big/ \int_0^{+\infty} E^4 T^{-2} e^{-E/T} dE \ .$$

In Eq. (1), *R* is *T* independent. This has been verified by measuring *R* for different input pulse powers as shown in Table I.

However, the good fit between the simple model above and our experimental results does not really demonstrate the validity of Anderson's suggestion [1

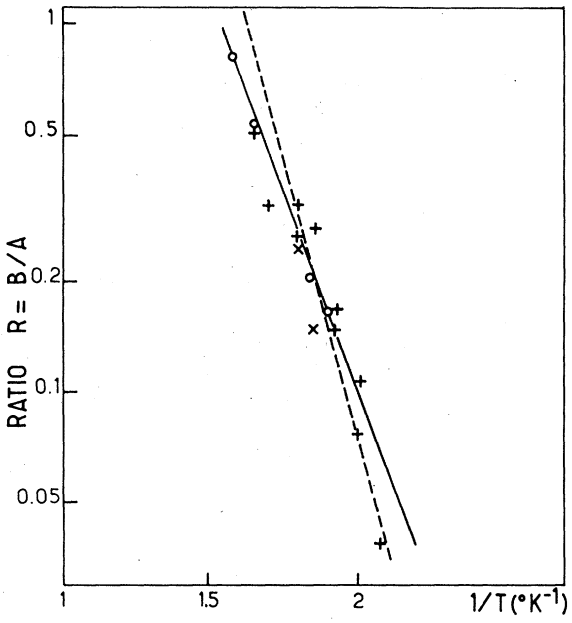

FIG. 3. Amplitude ratio $R = B/A$ of the signal due to atoms evaporated by phonons (*B*) to the direct phonon signal (*A*) as a function of inverse temperature (logarithmic scale). The notations (○, +, ×) correspond to various experiments. The solid line comes from Eq. (1). The dashed lines correspond to $R \propto e^{7.15/T}$.

TABLE I. Peak amplitude ratio $R = B/A$ of the signal due to atoms evaporated by phonons (B) to the direct phonon signal (A), measured at two different temperatures. R is power independent. The width of the input pulse is 1 μsec.

Power (mW)	$R = B/A$ at $T = 0.54$ °K	$R = B/A$ at $T = 0.56$ °K
80	0.13 ± 0.03	0.23 ± 0.04
45	0.12 ± 0.04	0.24 ± 0.05
20	0.15 ± 0.07	0.25 ± 0.07
10		0.3 ± 0.1

phonon (E) $\rightarrow$ 1 atom ($E - E_0$)].

Other models (for example two-phonon processes) could also lead to a variation of R near $e^{-7.15/T}$. A good test would be the observation of atoms evaporated by high-energy *ballistic* phonons. Unfortunately, we have not observed such a signal down to 0.12 °K.

One could think, after looking at the big signals due to atoms evaporated by rotons (next paragraph), that rotons still slightly coupled to the phonons could be responsible for the B signals shown in Fig. 2. But such a model would give a variation near $e^{-2\Delta/T}$ ($\Delta = 8.65$ °K is the roton-gap energy), because R would be proportional to the product of two quantities both proportional to $e^{-\Delta/T}$: the roton population and the rate of energy transfer from the phonon gas to the roton gas (which is itself proportional to the mean-phonon roton collision frequency).

Let us make a final remark. In Fig. 4 one can see the evolution of the direct-phonon signal as the temperature decreases down to 0.12 °K. We see mainly in this figure that the signal becomes sharper as the temperature decreases. This is characteristic of a propagation mode which becomes more and more ballistic. We are unable here to check the Maris prediction[11] of n second-sound modes. The result of this theory is hard to distinguish from that expected for ballistic phonons.[11]

In conclusion, we have observed evaporation from a phonon second-sound pulse. The temperature dependence and the power dependence of the evaporation is not in contradition with the very simple model described above. We have not observed evaporation from ballistic phonon, and thus no serious concluding model can be proposed.

IV. EVAPORATION BY ROTONS

One can see in Fig. 5 two typical recordings of the signal versus time obtained in the two situations A and B previously defined. As already mentioned in Sec. III, we observe a well defined sharp pulse of phonons in situation A, this is the phonon ballistic regime, but no evaporation. The only signal observed in situation B is due to atoms evaporated by rotons,

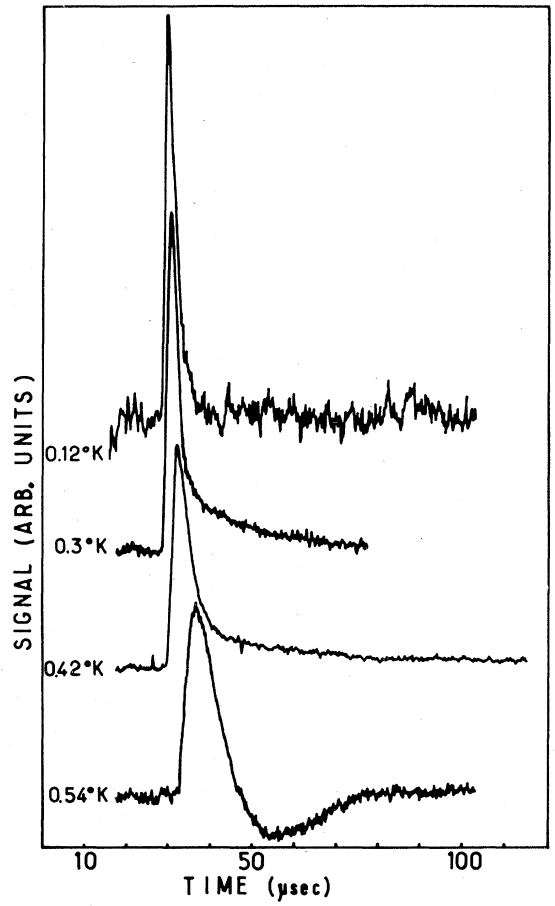

FIG. 4. Evolution of the direct phonon signal vs time as the temperature T decreases. The shape and arrival time at $T = 0.54$ °K denote the presence of a phonon second sound. At $T = 0.12$ °K, the ballistic phonon pulse is very sharp and propagates at the phonon velocity $c = 238$ m sec^{-1}.

and its amplitude is much larger than the direct roton signal in situation A (the sensitivity for the A signal is five times larger than for the B signal). This amplitude ratio seems anomalous, but it can be explained as follows. The coupling between rotons in liquid ^{4}He, and excitations in the solid detector, is small at standard vapor pressure.[12] Thus ballistic rotons are difficult to observe directly, and the A roton signal is small. On the contrary, in situation B, the probability for an incident evaporated atom to be trapped in the liquid film which covers the detector is of the order of unity.[4] Moreover, the film is very thin ($\sim$100 Å) and we think that the energy given to it by the incident flux of ^{4}He atoms is rapidly thermalized in the entire system (film plus detector). Thus, the apparent anomalous amplitude ratio between A and B signals only indicates that the small gas thickness, and the thin liquid film covering the detector in situation B, realize a kind of adaptation of the detector to the detection of rotons via their transformation into eva-

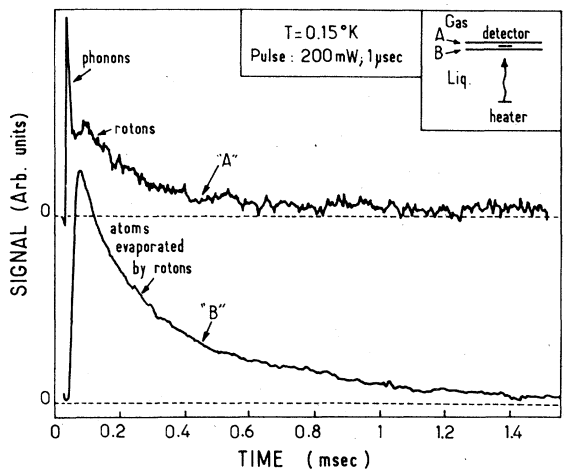

FIG. 5. Typical signals recorded at $T = 0.15$ °K with a Zn bolometer evaporated on a Si monocrystal. The B signal due to atoms evaporated by ballistic rotons has a much larger amplitude than the A one, due to direct detection of the rotons themselves. We do not observe atoms evaporated by phonons.

porated atoms. This is why we obtain well-defined signals due to rotons, and the possibility of measuring some of their properties in situation B.

Figure 6 shows five typical signals recorded at $T = 0.2$ °K for five different values of the liquid height x above the heater (the total heater-detector distance L is constant and equal here to 6.85 mm). On such

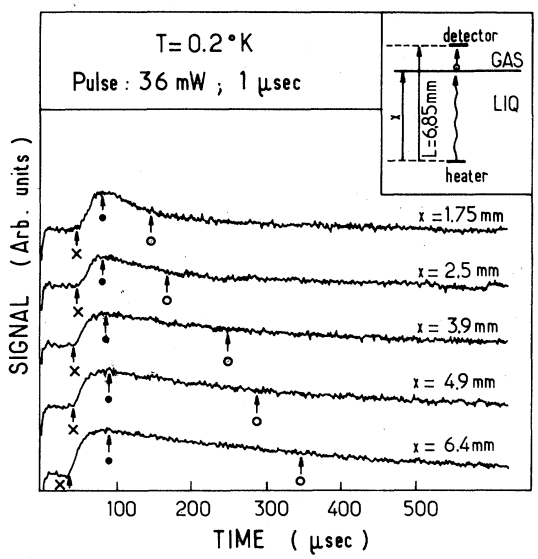

FIG. 6. Signal recorded vs time at $T = 0.2$ °K. The parameter x is the liquid height above the heater. The total heater-detector distance is $L = 6.85$ mm. The notations (×, •, ○) refer, respectively, to the starting edge, the maximum, and the half-height in the tail of the pulse.

curves, time-of-flight measurements and amplitude measurements lead to interesting information.

From time-of-flight measurements, the velocities, and therefore the energies of both rotons and atoms, can be inferred. Thus, we have been able to verify the energy conservation at the liquid-gas interface. We consider three different times (×, •, ○) corresponding, respectively, to the starting edge, the maximum, and the middle height in the tail of the signal. The same notations (×, •, ○) are used in Fig. 7(b) and plotted versus x. We first remark, in Fig.

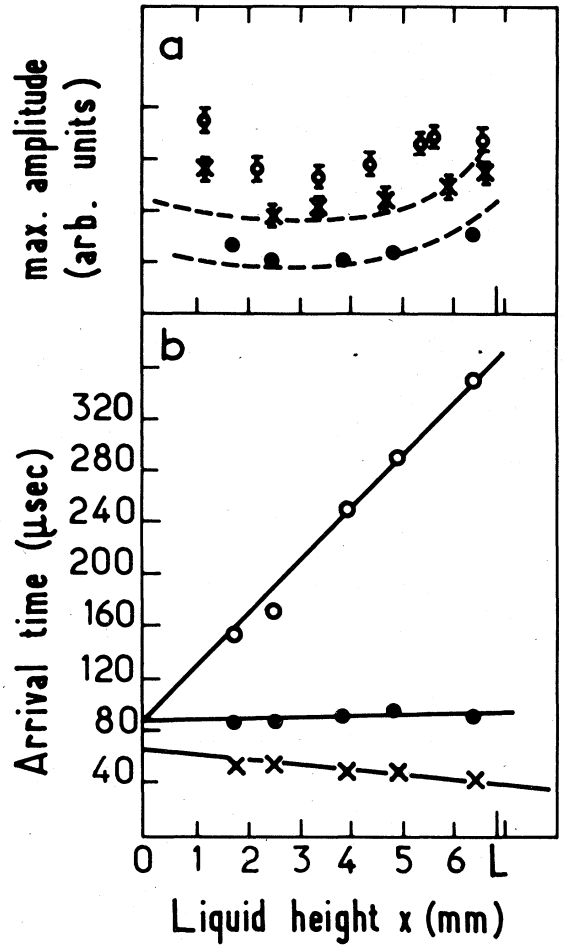

FIG. 7. Analysis of the arrival times (b) and of the maximum signal amplitude (a) vs x, the liquid height above the heater. (b) Arrival times (×, •, ○) are those of Fig. 6. Their variation with x is linear and in good accordance with Anderson's model. (a) Different points are, respectively, from the experiment shown on Fig. 6 (•) and two other experiments at 0.3 °K with different sensitivities (○ and ×). The amplitude variation always exhibits a minimum for $0 < x < L$. The two dashed curves come from Eq. (4) with two different values for the roton mean free path λ. ($\lambda = 3.1$ mm for the upper curve and $\lambda = 3.4$ mm for the bottom curve.)

7(b), that the variation of the three times is linear with the height x of the liquid. This confirms the ballistic character of the propagation of rotons at this temperature. (The vapor at this temperature is nearly vacuum and there is no doubt of the ballistic character of the propagation of the evaporated atoms.) The distribution of rotons created near the heater does not change very significantly during the propagation of the liquid. If the maximum of the signal, for example, corresponds to rotons with a velocity of 70 m sec^{-1} at a certain height x, the maximum always corresponds to the same rotons at a different height x. Each characteristic point of the pulse can be related to a definite roton propagating with constant velocity. Thus the slope of the line on Fig. 7(b) is positive if the rotons are slower than the atoms evaporated by them. It is negative if the rotons are faster. We obtain the energy of the rotons by taking the arrival time t at $x = L$, where L is the heater-to-detector distance with the relation

$$E_{\text{rotons}} = \Delta + \tfrac{1}{2}\mu(L/t)^2 \ , \qquad (2)$$

where $\Delta = 8.65$ °K is the roton gap energy, $\mu = 0.16$ m is the roton effective mass from the mass m of a helium atom, $L = 6.85$ mm is the heater-detector distance. We obtain the kinetic energy of the atoms evaporated by rotons by taking the arrival time for $x = 0$ with a relation of the same kind

$$E_{\text{atoms}} = \tfrac{1}{2}m(L/t)^2 \ . \qquad (3)$$

Let us now return to the predictions of Anderson[2]; he considers only elastic single-particle emission, a process like

$$1 \text{ roton}(E) \rightarrow 1 \text{ atom}(E - E_0) \ .$$

One can see in Fig. 8 the excitation spectrum of superfluid ^{4}He: the roton minimum energy Δ is 1.5 °K above the binding atomic energy $E_0 = 7.15$ °K. Thus

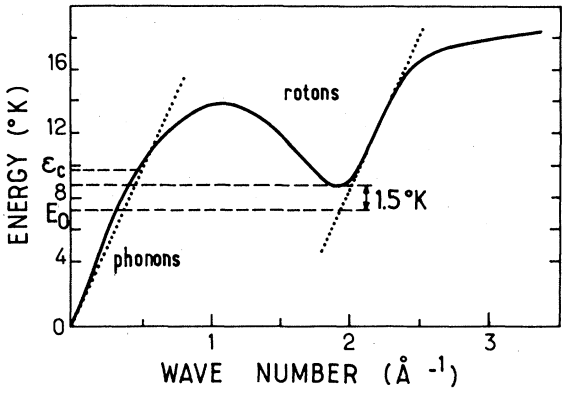

FIG. 8. Dispersion curve for superfluid ^{4}He. The anomalous dispersion of the phonon part has been amplified. $\epsilon_c = 9.5$ °K is the critical energy associated with this anomaly (Ref. 16). $\Delta = 8.65$ °K is the roton minimum energy. $E_0 = 7.15$ °K is the atomic binding energy in the liquid. $\Delta - E_0 = 1.5$ °K is the minimum kinetic energy of atoms evaporated by rotons.

atoms evaporated by rotons in such a process have a minimum kinetic energy of 1.5 °K, and their arrival time extrapolated at $x = 0$ must be less than 86 μsec in our case [relation (3)]. This is precisely one of the results shown in Fig. 7(b). The complete study of the energy conservation in the evaporation process predicted by Anderson is summarized in Table II. One sees that the agreement between Anderson's predictions and our experimental results is very good. For the three considered points we get the same energy from the arrival time of rotons ($x = L$) and the arrival time of the corresponding evaporated atoms ($x = 0$). It is a demonstration of the validity of one of Anderson's ideas: there is an evaporation process corresponding to elastic single-atom emission by single rotons.

TABLE II. Comparisons of the kinetic energy of atoms to the energy of the rotons which have evaporated them. The experimental result is in accordance with Anderson's prediction of an elastic emission like 1 roton (E) $\rightarrow$ 1 atom ($E - \Delta + 1.5$). Experimental conditions: $T = 0.2$ °K; pulse: 36 mW, 1 μsec; heater-detector: 6.85 mm.

Considered point on the signal	Starting edge (×)	Maximum (•)	Half-height (○)
t for $x = 0$ (μsec)	66	84	86
$V_{\text{atoms}} = L/t$ (msec)	103	82	79
$E_{\text{atoms}} = \frac{1}{2}m(L/t)^2$ (°K)	2.5	1.56	1.5
t for $x = L$ (μsec)	42	96	370
$V_{\text{rotons}} = L/t$ (m sec^{-1})	161	70	18.5
$E_{\text{rotons}} - \Delta = \frac{1}{2}\mu(L/t)^2$ (°K)	0.98	0.19	0.013
$E_{\text{rotons}} - \Delta + 1.5$ (°K)	2.48	1.69	1.51

Amplitude measurements are also interesting because the amplitude of the signal is related to the number of rotons coming up to the free surface, i.e., to their mean free path. We have plotted on Fig. 7(a) the maximum amplitude of the signal versus x for three different sets of curves. We always obtain the same behavior: there is a minimum amplitude for an intermediate value of the liquid height x between $x=0$ and $x=L$.

This gives us an estimation of the roton mean free path λ as follows. The amplitude varies as a function of x, following two conflicting conditions. The propagation of rotons is ballistic but their mean free path is not infinite (a minimum mean number of ~25 collisions between the heater and the detector is necessary to construct a second-sound wave[9]). Thus the amplitude of the signal must decrease as x increases like $e^{-x/\lambda}$, but there is also a geometrical effect: because of the finite dimensions of the heater and the detector, there is an efficient angle of emission. What goes on at the liquid-gas interface? A roton near the minimum Δ has a momentum of about 2 Å^{-1}. A ^{4}He atom with kinetic energy 1.5 °K has a momentum of about 0.5 Å^{-1}. The conservation of transverse momentum then induces an opening of the useful angle at the interface by a factor of about 4. The effect of this opening on the amplitude of the signal is easy to calculate and gives finally a total variation of the amplitude A like

$$A \propto (L-\tfrac{3}{4}x)^{-2}\exp(-x/\lambda) \quad . \tag{4}$$

This expression exhibits a minimum for $0<x<L$ only if $\frac{1}{6}L<\lambda<\frac{2}{3}L$, i.e., $1<\lambda<5$ mm. The two dotted lines in Fig. 7(b) are deduced from Eq. (4) with two different values of λ: 3.1 mm (upper line, experimentat at 0.3 °K) and 3.4 mm (bottom line, experiment at 0.2 °K). These two values can, in fact, be summarized by a single value $\lambda=3\pm2$ mm. The fit between Eq. (4) and our experimental points is not sufficiently good to allow us to perform a complete analysis of λ as a function of both roton energy E and ambient temperature T. We think, however, that this is one of the most direct experimental measurements of the roton mean free path. The obtained value ($\lambda=3\pm2$ mm at $T=0.2$ °K for rotons of 70 m sec^{-1}) seems in reasonable agreement with calculations on roton-roton collisions[7] and roton-^{3}He collisions.[13]

V. OBSERVATION OF A MAXIMUM ROTON VELOCITY

In Fig. 9 one can see different signals recorded at different temperatures and pulse powers. The liquid-gas interface is just below the detector (less than 50 μm, situation labeled B in Sec. III). Thus, as shown in Sec. IV, each point of the signal at time t can be related to a roton traveling without collisions from the heater up to the free surface, with a velocity L/t and energy E given by Eq. (2). We mainly remark in Fig. 9 that the arrival time of the signal maximum (arrows) is power and temperature dependent, whereas that of the starting edge (dashed line) is not.

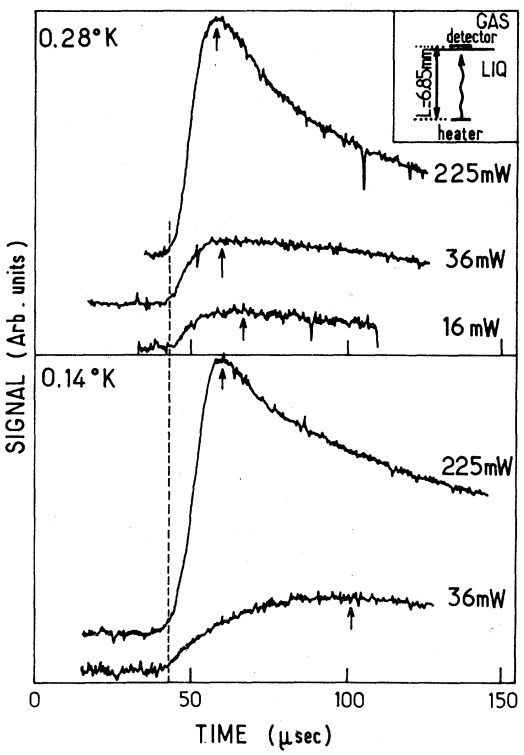

FIG. 9. Signal due to atoms evaporated by rotons, for various ambient temperatures and various pulse powers. The starting edge of the detected pulses is power and temperature independent (dashed line), not the maximum (arrows). The heater-detector distance is 6.85 mm and the liquid-level–detector distance less than 50 μm.

The dashed line corresponds, for a distance $L=6.85$ mm, to a maximum roton velocity $v=160\pm10$ m sec^{-1} (or a maximum roton energy $E=9.6\pm0.2$ °K). This surprising result leads to the following analysis.

Let us suppose that the distribution of emitted rotons is thermal (i.e., with an occupation probability like e^{-E/T_e}, where T_e is an "effective-emission temperature"). This is an approximation, but illustrates quite well the behavior of the signal maximum.

One can easily calculate that, with this assumption, the signal maximum corresponds to rotons of kinetic energy $\frac{1}{2}\mu v^2=T_e$, so that

$$T_e=\tfrac{1}{2}\mu(L/t_M)^2 \quad , \tag{5}$$

where t_M is the arrival time of the signal maximum and we obtain the values shown on Table III.

T_e is more dependent on the pulse power at 0.14 °K

TABLE III. Estimation of an effective roton-emission temperature for the different curves of Fig. 9. The estimation is made supposing a thermal distribution of rotons and using Eq. (5).

Ambient temperature (°K)	Pulse power (mW)	Estimated effective emission temperature (°K) [Eq. (5)]
0.28	225	0.52
0.28	16	0.4
0.14	225	0.5
0.14	36	0.22

than at 0.28 °K and this seems very reasonable: for a 225-mW pulse power, T_e is about 0.5 °K and tends to the ambient temperature (0.28 or 0.14) as the pulse power goes to zero. The absolute value of T_e also seems reasonable if we refer to the estimation by Narayanamurti.[14] Finally, the absolute position and variation of the maximum is not surprising.

In constrast, the arrival time of the edge is constant. This indicates the presence of some physical mechanism which cuts the spectrum of the detected rotons at a value of 160 m sec^{-1} for the velocity ($\Delta + 1 = 9.6$ °K for the energy). We do not have a definite explanation for this cutoff but let us critically examine some possibilities.

(a) Pitaevskii[15] suggested an interaction process between rotons and phonons when the roton group velocity reaches that of phonons (238 m sec^{-1}). This process should cut the observed roton spectrum at a value near 238 m sec^{-1}, not at 160 m sec^{-1} as we obtain here.

(b) Following Tan *et al.*,[13] the ^{3}He-roton scattering cross section is smaller for rotons of momentum $p < p_0$ than for rotons with $p > p_0$ (p_0 is the momentum of rotons with minimum energy Δ). If the ^{3}He-roton collisions are dominant, this means that the rotons observed in our experiment should be mostly from the ($p < p_0$) branch, where the maximum value of the velocity is about 135 m sec^{-1}.

(c) The first two explanations concern the propagation in the liquid and lead to an energy-dependent roton mean free path, but the observed cutoff is perhaps related to the evaporation of atoms at the free surface. The cutoff energy (9.6 °K) lies near the critical energy ($\epsilon_c = 9.5$ °K, see Fig. 8) for the anomalous dispersion of phonons.[16] Can a strong variation of the phonon lifetime near ϵ_c induce some variation of the probability for a roton of the same energy to evaporate an atom?

We think that the interpretation of this last experimental result is a very open problem.

VI. CONCLUSION

Using the heat-pulse technique, we have studied the evaporation of superfluid ^{4}He. Two microscopic evaporation processes are observed. One is due to phonons, the other, due to rotons, is in very good agreement with Anderson's prediction of a single-particle elastic emission. Various experimental results on the excitations in the liquid have also been obtained. We measured especially the mean free path of rotons and a surprising maximum value of the roton group velocity.

ACKNOWLEDGMENTS

We would like to thank J. P. Maneval and his collaborators for their support during the course of this work.

*Laboratoire associé au Centre National de la Recherche Scientifique.

[1]W. D. J. Johnston and J. G. King, Phys. Rev. Lett. 16, 1191 (1966); and Bull. Am. Phys. Soc. 17, 38 (1972).

[2]P. W. Anderson, Phys. Lett. A 29, 563 (1969).

[3]S. Balibar, Phys. Lett. A 51, 455 (1975).

[4]D. O. Edwards, P. Fatourous, G. G. Ihas, P. Mrozinski, S. Y. Shen, F. M. Gasparini, and C. P. Tam, Phys. Rev. Lett. 34, 1153 (1975).

[5]C. Caroli, B. Roulet, and D. Saint James, Phys. Rev. B 13, 3875 (1976).

[6]D. T. Meyer, H. Meyer, W. Hallidy, and C . F. Kellers, Cryogenics 3, 150 (1963).

[7]I. M. Khalatnikov and D. M. Chernikova, Sov. Phys.-JETP 22, 1336 (1966).

[8]The roton propagation is slower and dispersive, leading to a pulse arriving later with a very broadened shape. (A long tail at long time is related to very slow rotons with energy near the minimum Δ where the roton group velocity is zero.) This can be seen in Ref. 3 or in Fig. 5 here.

[9]V. Narayanamurti, R. C. Dynes, and K. Andres, Phys. Rev. B 11, 2500 (1975).

[10]R. W. Guernsey, K. Lusczynski, and W. C. Mitchell, Cryogenics 7, 110 (1967); B. Castaing, Phys. Rev. B 13, 3854 (1976).

[11]H. J. Maris. Phys. Rev. A 9, 1412 (1974); and private communication.

[12]F. W. Sheard, R. M. Bowley, and G. A. Toombs, Phys. Rev. A 8, 3135 (1973). T. J. Sluckin, F. W. Sheard, R. M. Bowley, and G. A. Toombs, J. Phys. C 8, 3521 (1975).

[13]H. T. Tan and Chia-Wei-Woo, Phys. Rev. Lett. 30, 365 (1973).
[14]R. C. Dynes and V. Narayanamurti, Phys. Rev. B 12, 1720 (1975).
[15]L. P. Pitaevskii, Sov. Phys.-JETP 9, 830 (1959).
[16]V. Narayanamurti and R. C. Dynes, Phys. Rev. B 13, 2898 (1976); A. F. G. Wyatt, N. A. Lockerbie, and R. A. Sherlock, Phys. Rev. Lett. 33, 1425 (1974).